Electronic supplementary information (ESI)

Mesoporous carbon nitride supported 5,10,15,20-tetrakis(4-methoxyphenyl)-21H,23H-porphine cobalt(II) as a selective and durable electrocatalyst for the production of hydrogen peroxide *via* two-electron oxygen reduction

Devesh Kumar Singh, Vellaichamy Ganesan,* Dharmendra Kumar Yadav, Mamta Yadav, Piyush Kumar Sonkar, and Rupali Gupta

Department of Chemistry, Institute of Science, Banaras Hindu University

Varanasi-221 005, UP, India

Telephone: +91-542-2307321; Fax : +91-542-2368127

E-mail: velganesh@yahoo.com and velgan@bhu.ac.in

* Corresponding author

Synthesis of mesoporous carbon (MPC) and CoTMPP integrated MPC

Mesoporous carbon was synthesized using similar experimental as used for the MCN synthesis. Sucrose was used as the carbon source and an equal amount of carbon content was maintained in the precursor as that used in the synthesis of MCN.

Experimental details for ICPE measurements

An accurately weighed amount of CoTMPP@MCN is treated with concentrated HNO_3. This process leaches out CoTMPP from the CoTMPP@MCN into the solution. Assuming a complete dissolution of CoTMPP into the solution, the solution obtained after filtration is used as the working solution for the ICPE measurements. For ICPE measurement after the stability test, the material was scratched out from the working electrode (indium tin oxide coated quartz plate for this current experiment) and used after the above treatment with concentrated HNO_3.

Determination of electrochemically active surface area (ECSA)

Cyclic voltammetry (CV) response for the GC/CoTMPP@MCN and GC/MCN electrodes were recorded at different scan rates (20, 40, 60, 80, 100, 120, 140, 160, 180, 200 mV/s). The potential range is chosen in the region, where there is no faradic process and charging of the double layer is the only possible process. From the CV measurements, a plot between anodic current (at 0.92 V (*vs*. RHE)) and scan rate is made and the slope of this plot gives the value of double layer capacitance (C_{dl}). The ECSA of the modified electrodes were obtained using the relation S1

ECSA= C_{dl} (modified electrode)/C_{dl} (GC)   S1

C_{dl} for bare glassy carbon (GC) electrode is found to have values in the range of 20 - 60 μFcm^{-2} per cm^2 of ECSA.[S1,S2] In the present calculation, 60 μFcm^{-2} per cm^2 of ECSA as C_{dl} of plane GC is used.

Determination of the roughness factor

The roughness factor of the electrode is the ratio of ECSA to the geometrical surface area of the electrode. Roughness factor values for modified electrodes were calculated and tabulated in Table S1

Determination of faradic efficiency of H_2O_2 formation

Faradic efficiency (FE) was determined based on the charge consumed and the actual amount of H_2O_2 produced. The charge consumed was obtained directly from the amperometric data and the amount of H_2O_2 produced was measured using the volumetric titration method.

Titration procedure

The amperometric analysis was carried out at an applied potential of 0.043 and 0.50 V (*vs*. RHE) in 0.1 M $HClO_4$ and 0.1 M KOH respectively, for 3600 s. At an interval of 1200 s, 1.0 mL of the electrolyte was taken and 1.0 mL of KI solution (2 wt%) was added. In the resulting mixture, 1.0 mL of 3.5 M H_2SO_4 and 50 μL of molybdate indicator (prepared by mixing 0.5 g ammonium molybdate and 1.5 g of ammonium nitrate in 5 mL of 6 M NH_4OH and making up to 25 mL by water) was added and titrated against 1.0 mM sodium thiosulphate solution. The calculated faradic efficiencies are tabulated below (Table S2).

Calculation of turn over frequency (TOF)

The number of active sites on the electrodes was calculated using a reported procedure.[S3] Briefly, the CV response of GC/CoTMPP@MCN was recorded in nitrogen saturated 0.1 M KOH solution. The potential range is chosen in such a way that in the selected region no catalysis occurs (0.87 to 1.27 V *vs.* RHE). The CV response (Figure S6) is integrated to calculate the charge consumed and the number of active sites (n) is calculated using equation S2.

$$n = \frac{Q}{2F} \qquad\qquad …(S2)$$

Then the TOF was calculated based on the amount of H_2O_2 produced (equation S3, Table S3).

$$TOF \quad = \quad \frac{\text{amount of H2O2 produced } (\frac{mol}{s})}{number\ of\ active\ sites\ (mol)} \qquad …(S3)$$

Table S1. Number of electrons involved in the ORR at CoTMPP@MCN, CoTMPP@MPC, and CoTPP@MCN in both acidic and basic media at different potentials.

Material	Number of electrons (n) (Potential)	
	0.1 M KOH	0.1 M HClO$_4$
CoTMPP@MCN	n= **1.8** (0.37 V)	n= **1.9** (-0.032 V)
	n= **1.8** (0.39 V)	n= **2.1** (-0.042 V)
	n= **1.9** (0.41 V)	n= **2.1** (-0.052 V)
	n= **1.7** (0.43 V)	n= **2.0** (-0.062 V)
	n= **2.0** (0.45 V)	n= **2.1** (-0.072 V)
CoTMPP@MPC	n= **3.4** (0.18 V)	n= **3.3** (0.0 V)
	n= **3.9** (0.28 V)	n= **3.4** (-0.1 V)
	n= **3.5** (0.38 V)	n= **3.5** (-0.2 V)
	n= **3.7** (0.48 V)	n= **3.4** (-0.3 V)
CoTPP@MCN	n= **3.7** (0.15 V)	n= **3.3** (0.0 V)
	n= **3.5** (0.25 V)	n= **3.4** (-0.1 V)
	n= **3.7** (0.30 V)	n= **3.1** (-0.2 V)
	n= **3.4** (0.35 V)	n= **3.3** (-0.3 V)

Table S2. Roughness factor of the modified electrodes

Electrode	Roughness factor	
	in 0.1 M $HClO_4$	in 0.1 M KOH
GC/MCN	2.1	3.3
GC/CoTMPP@MCN	3.6	5.0

Table S3.   Faradic efficiency of CoTMPP@MCN for H_2O_2 formation.

Medium	Time (s)	Charge consumed (C)	Theoretical H_2O_2 (μ mole)	Experimentally measured H_2O_2 (μ mole)	Faradaic efficiency (%)	Average Faradaic efficiency (%)
HClO$_4$ (0.1 M)	1200	0.026	0.14	0.12	85.7	87.6
	2400	0.054	0.28	0.24	85.7	
	3600	0.068	0.35	0.32	91.4	
KOH (0.1 M)	1200	0.066	0.34	0.30	88.2	89.0
	2400	0.128	0.66	0.58	87.8	
	3600	0.172	0.89	0.76	91.0	

Table S4. Parameters obtained from the best fit Randle's equivalent circuit for the impedance data

Sample	R_s (ohm)	Q_1 (F)	R_{ct} (ohm)	Q_2 (F)	R_p (ohm)
MCN	90.77	3.81	2328	0.00127	5.6×10^{12}
CoTMPP@MCN	95.69	2.11	1610	0.00056	6.0×10^{10}
CoTMPP	91.02	0.8	2004	0.00009	461.2
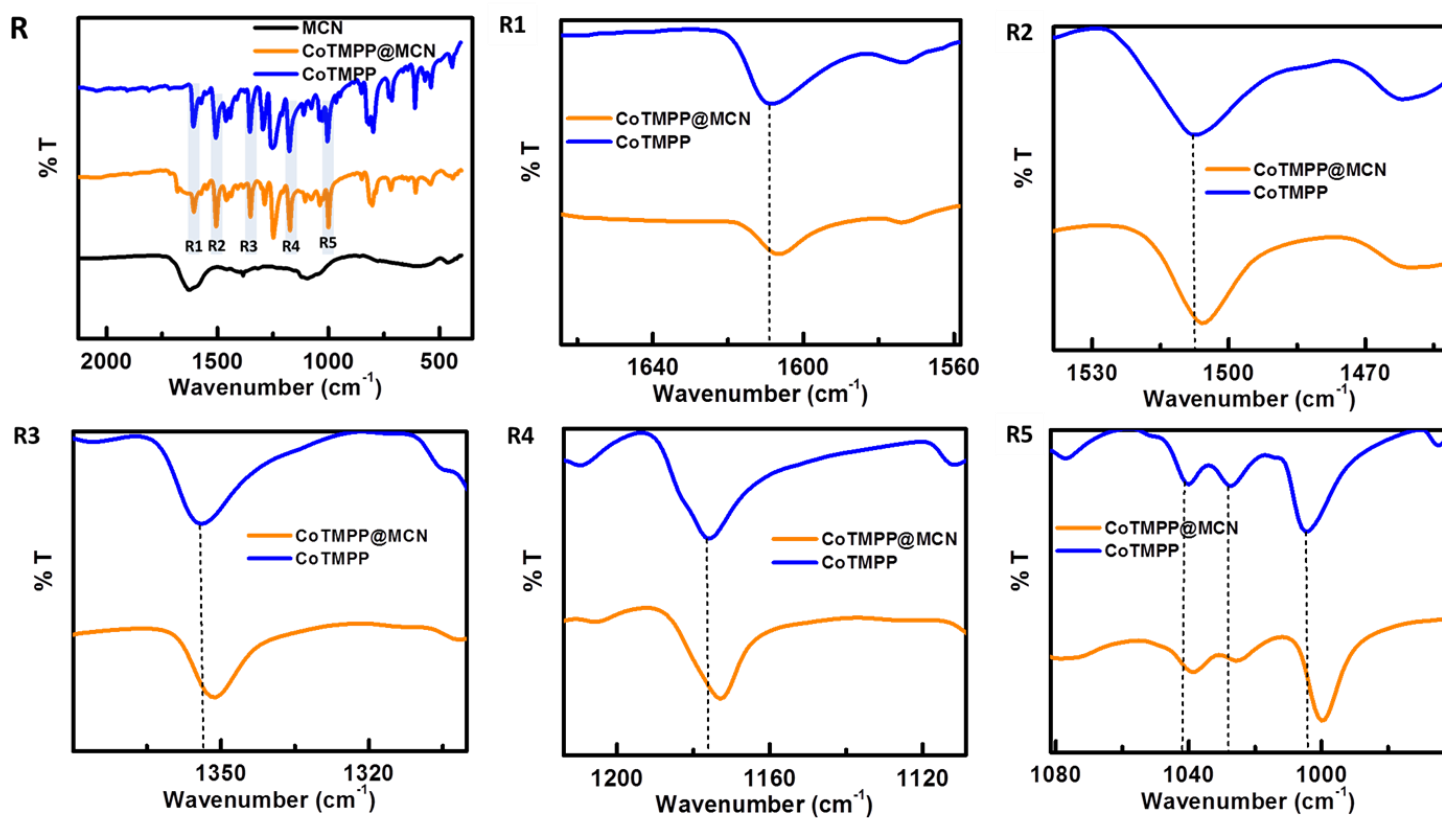
Figure S1   FT-IR spectra of MCN, CoTMPP@MCN, and CoTMPP (R) with enlarged highlighted regions, R1-R5.
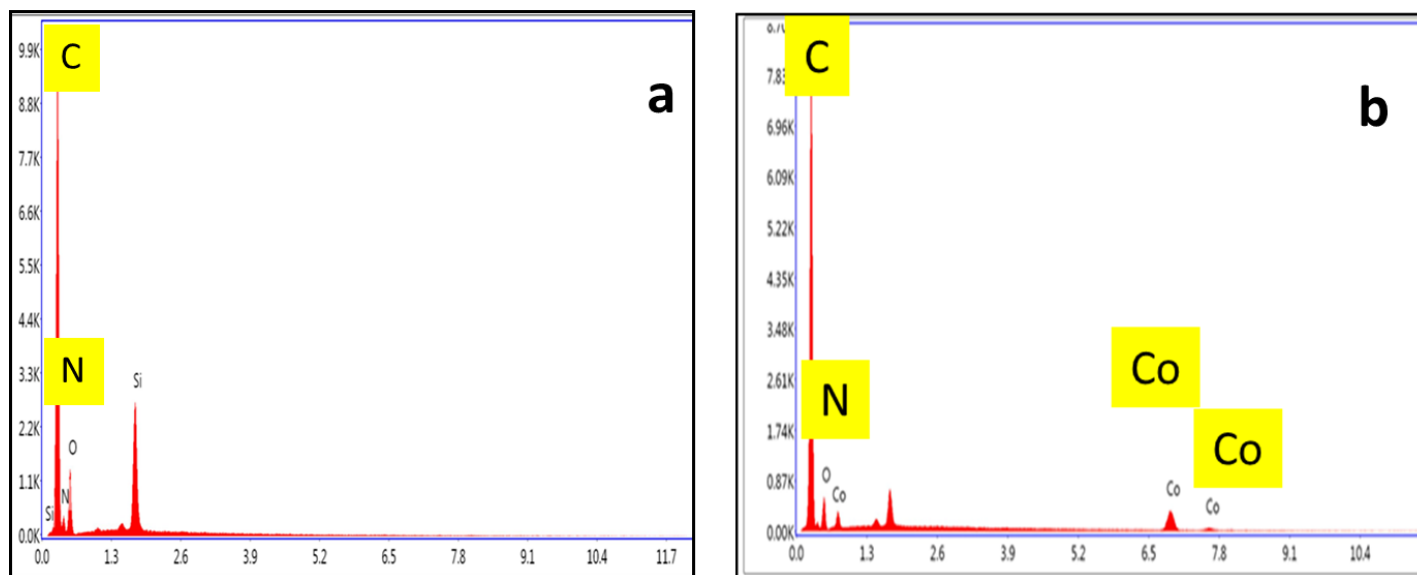
Figure S2   EDAX spectra of MCN (a) and CoTMPP@MCN (b).
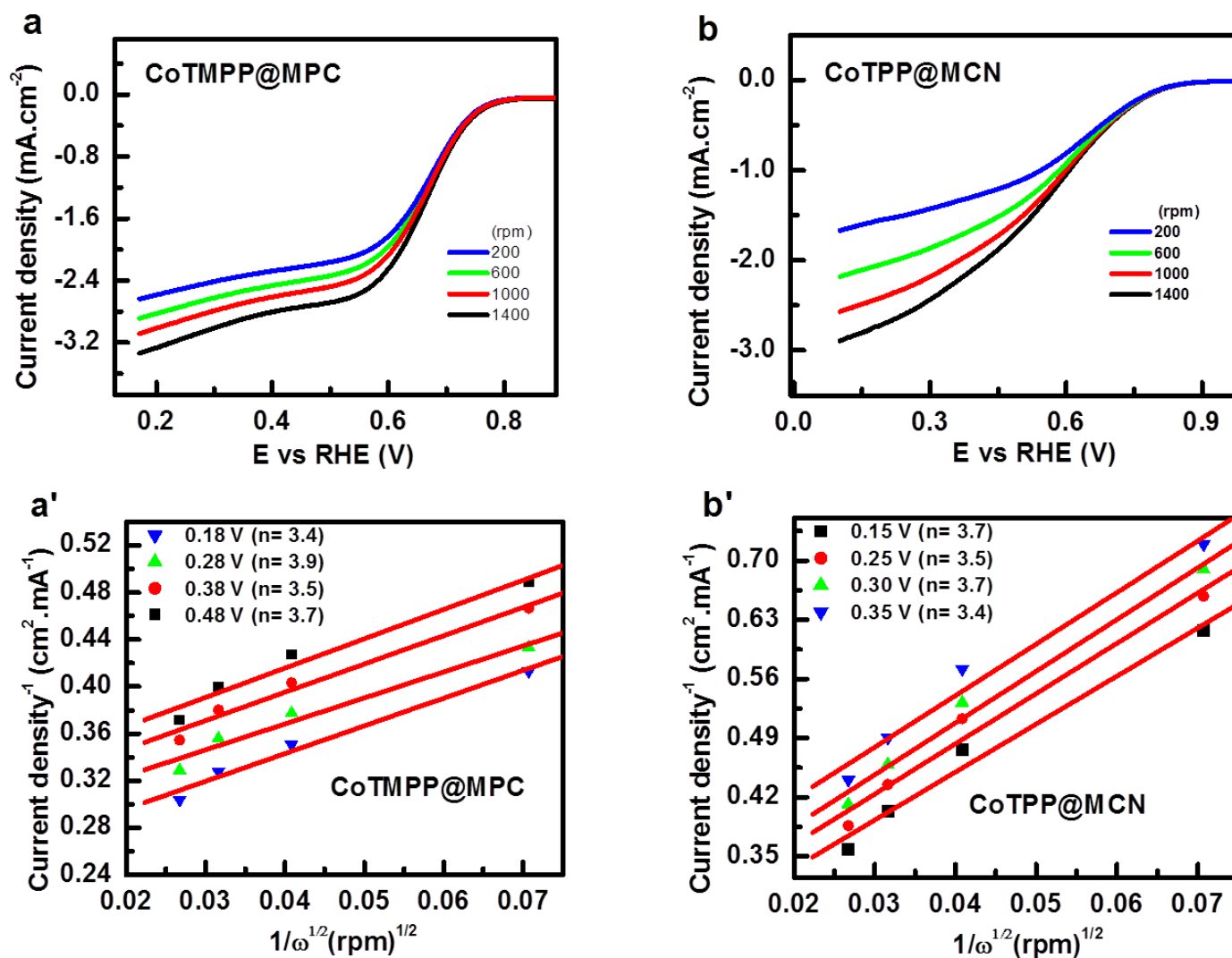
Figure S3 LSV responses at increasing rotation rate for CoTMPP@MPC (a) and CoTPP@MCN (b) in oxygen saturated 0.1 M KOH. K-L plot derived from the LSV response for CoTMPP@MPC (a') and CoTPP@MCN (b').
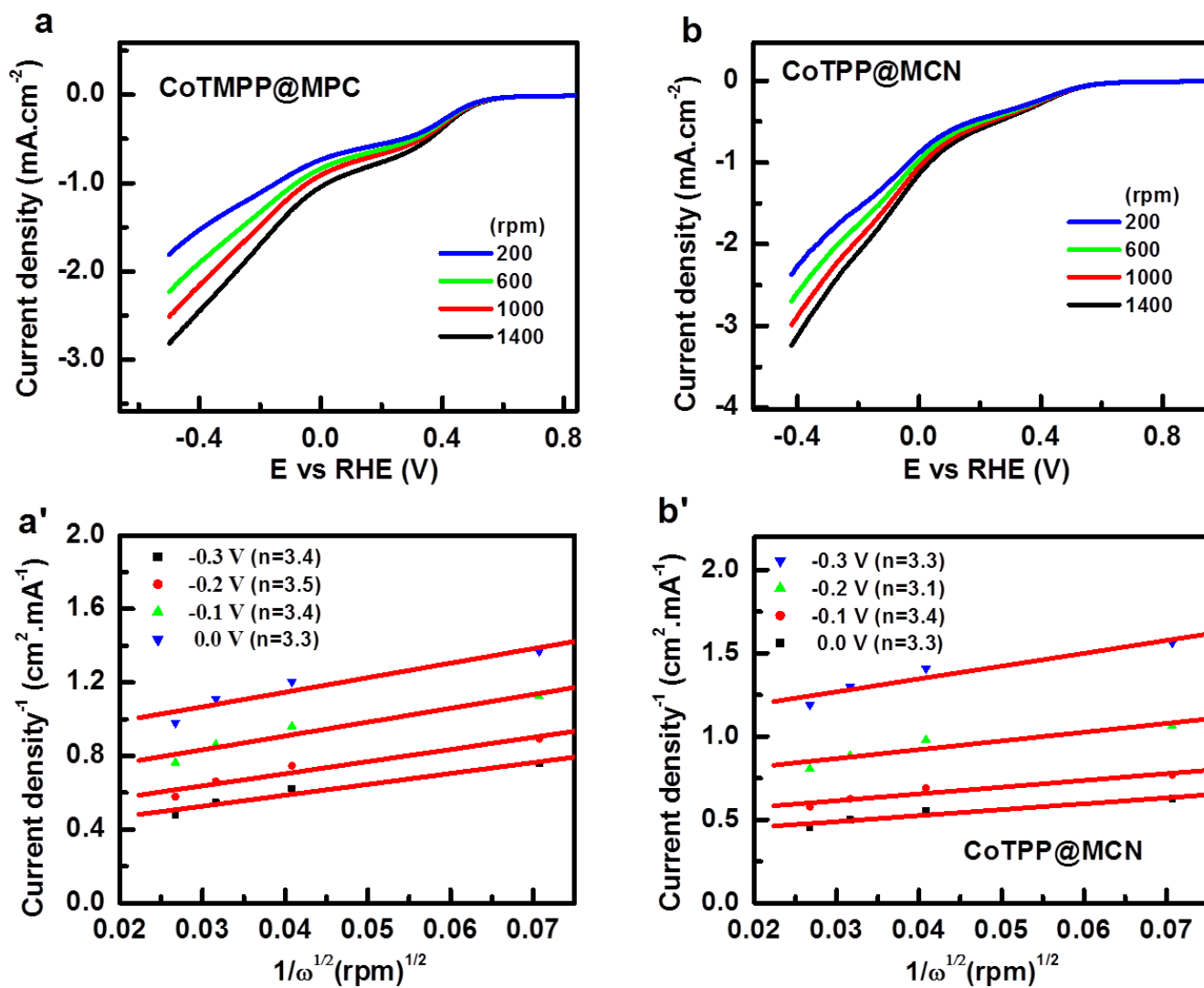
Figure S4 LSV responses at increasing rotation rate for CoTMPP@MPC (a) and CoTPP@MCN (b) in oxygen saturated 0.1 M $HClO_4$. K-L plot derived from the LSV response for CoTMPP@MPC (a') and CoTPP@MCN (b').
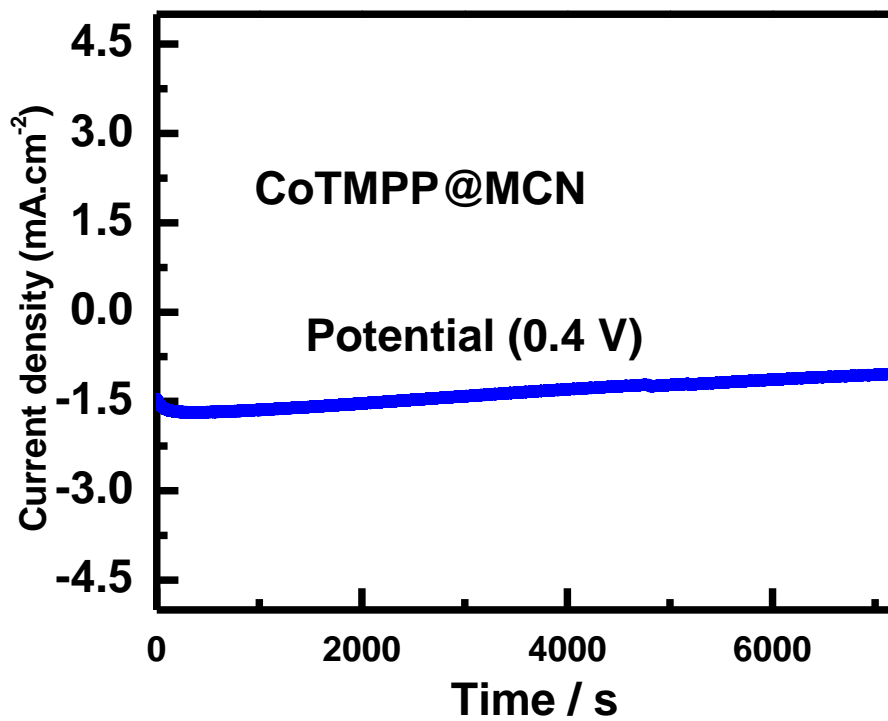
Figure S5   Amperometric i-t response of GC_{RDE}/CoTMPP@MCN in 0.1 M KOH at an applied potential of 0.4 V (*vs.* RHE) and a rotation rate of 1600 rpm.
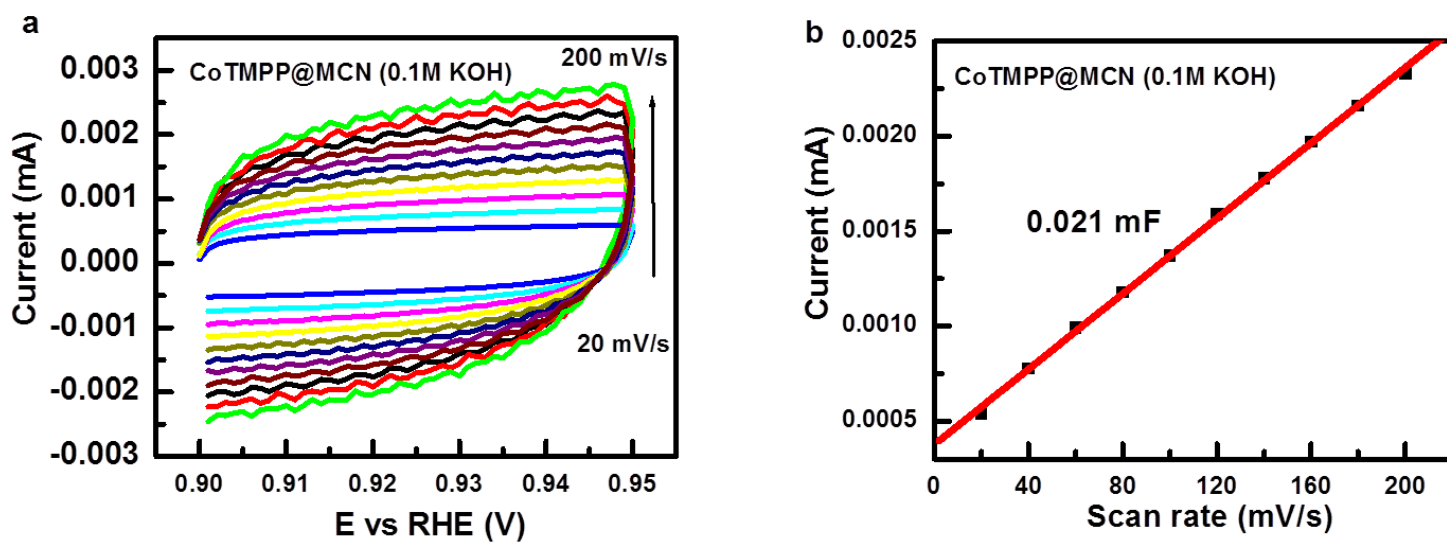
Figure S6   CV responses of GC/CoTMPP@MCN at different scan rates (a) and the corresponding anodic current *vs.* scan rate plot (b) before the amperometric analysis.
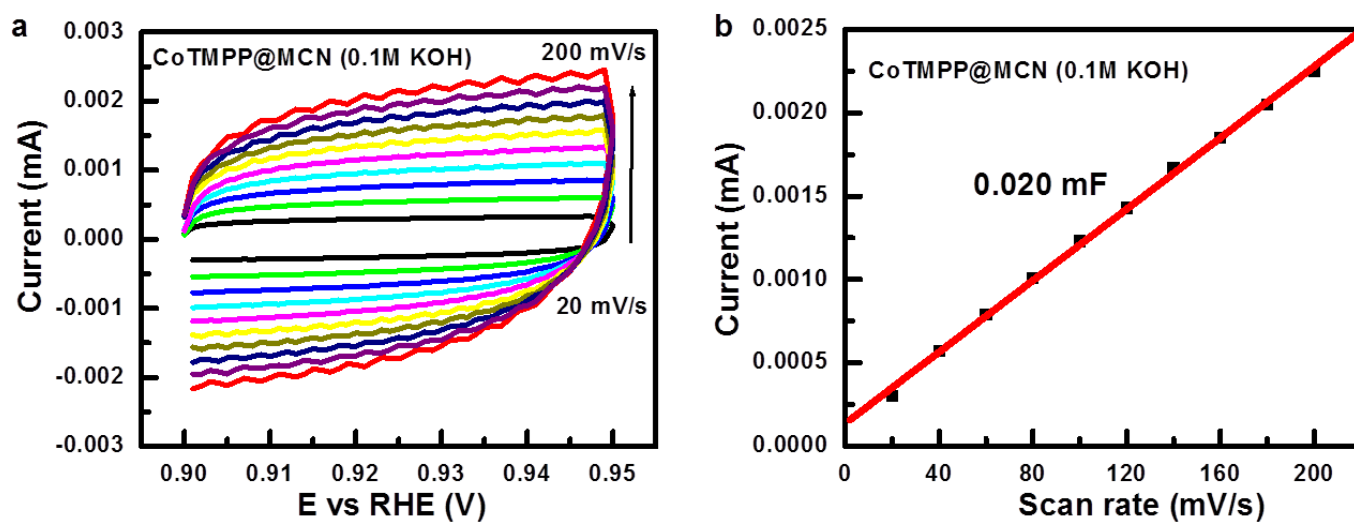
Figure S7   CV responses of GC/CoTMPP@MCN at different scan rates (a) and the corresponding anodic current *vs.* scan rate plot (b) after the amperometric analysis.
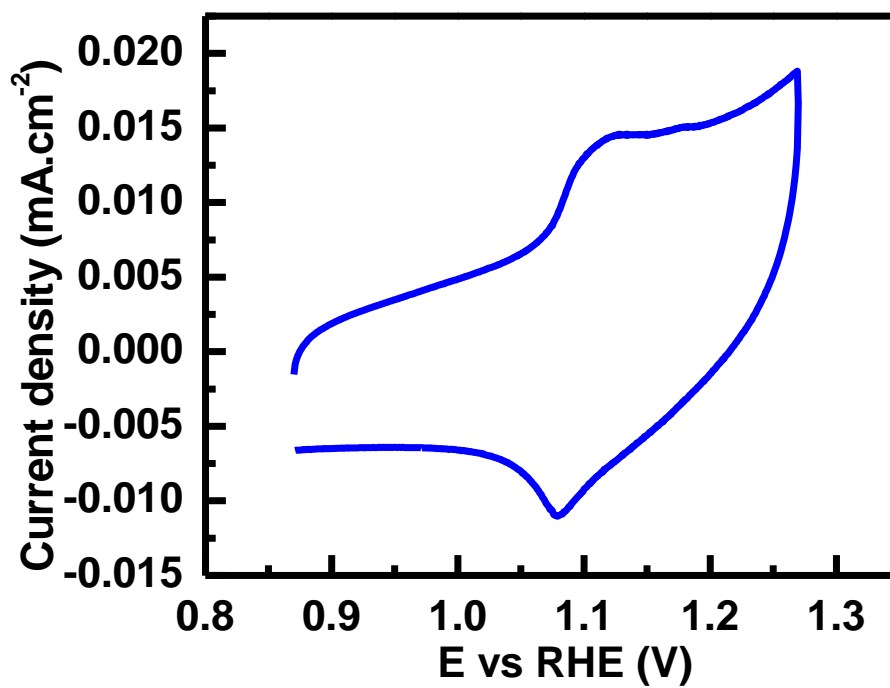
Figure S8   CV response of GC/CoTMPP@MCN in nitrogen saturated 0.1 M KOH. Scan

rate: 300 mVs[-1]

References

(S1) H. Deng, C. Zhang, Y. Xie, T. Tumlin, L. Giri, S. P. Karnab, J. Lin, *J. Mater. Chem. A* **2016**, 4, 6824.

(S2) C. Zhang, Y. Shi, Y. Yu, Y. Du, B. Zhang, *ACS Catal.* **2018**, 8, 8077.

(S3) S. Anantharaj, S. R. Ede, K. Karthick, S. S. Sankar, K. Sangeetha, P. E. Karthik, S. Kundu, *Energy Environ. Sci.* **2018**, 11, 744.